scientific reports

Check for updates

OPEN

A proposed methodology for mollification of subsynchronous oscillation in DFIG-based wind farm

Mohamed Abdeen[1], Mahmoud A. El-Dabah[1]✉ & Ahmed M. Agwa[2]

High levels of series compensation in transmission lines, particularly those integrated with wind farms, exacerbate the risk of sub-synchronous oscillation (SSO), a phenomenon detrimental to system stability. Gate-controlled series capacitor (GCSC) is one of the used means to mitigate the SSO and enhance power transfer capability. In the previous studies, the combined proportional-integral controller with supplementary damping controller was an effective approach for controlling the GCSC and mitigating the SSO. In this paper, the ability to cascade a proportional-resonant controller with a PI controller for damping the SSO is investigated. The proposed method's performance is evaluated through extensive time-domain simulations using the modified IEEE First benchmark model. The simulations incorporate a diverse range of wind speeds, compensation levels, as well as sub-synchronous control interactions. Furthermore, a comparative analysis with recent SSO damping techniques is conducted to assess the strategy's performance under varying operating conditions. The comparative results overwhelmingly demonstrate the superiority and effectiveness of the proposed strategy in alleviating SSO, especially at low wind speeds and high compensation levels.

Keywords Series compensated transmission lines, Sub-synchronous oscillation, Gate-controlled series capacitor, Proportional resonant, Supplementary damping control

The rapid expansion of renewable energy generation, driven by dwindling fossil fuel reserves and surging energy consumption, necessitates innovative solutions for grid integration. Among these renewables, wind energy stands out as the most prevalent source. However, transmitting the power generated by geographically dispersed wind farms to consumption centers often requires high-voltage transmission lines. Series capacitors are strategically employed within these lines to augment power transfer capability[1]. While increasing the compensation level (reducing series capacitor reactance) enhances power transfer, it inadvertently creates conditions conducive to sub-synchronous oscillation (SSO)[2,3]. This phenomenon, if not adequately mitigated, can compromise grid stability, posing a significant challenge to the seamless integration of wind energy into power systems[4,5]. Upon examination, it is discerned that such SSO shares similarities with the induction-generator effect (IGE). The activation of IGE occurs when the rotor's negative resistance surpasses the total network resistance at a frequency lower than the rated system frequency, specifically, at sub-synchronous frequency[6]. The manifestation of this IGE may occur in a wind plant-based doubly fed induction generator (DFIG) integrated with a fixed series capacitor transmission line, contingent upon the level of series compensation and wind speed[7]. It is noteworthy that SSO extends beyond the confines of IGE, encompassing diverse facets such as torsional interaction (TI), torque amplification (TA), sub-synchronous control interaction (SSCI), and sub-synchronous torsional interaction (SSTI)[8]. Among these, the DFIG stands out as the most prevalently employed, owing to its proficiency in harnessing maximum power across variable wind speeds. In the context of a DFIG-based wind turbine, the principal types of SSO are ascribed to SSCI and IGE. The impact of the rotor-side converter (RSC) and grid-side converter (GSC) parameters on the system stability have been investigated in Ref[9]. It was proven that the RSC parameters affect the system stability, where the higher the parameters of RSC, the lower the system stability. That is to say that increasing the RSC parameters has an adverse impact on the system stability. On the other hand, the parameters of the GSC don't influence system stability[9].

[1]Electrical Engineering Department, Faculty of Engineering, Al-Azhar University, Cairo, Egypt. [2]Department of Electrical Engineering, College of Engineering, Northern Border University, Arar, Saudi Arabia. ✉email: Dr_mdabah@azhar.edu.eg

Failure to implement timely measures to prevent SSR may lead to various consequences, including the loss of generated power, equipment damage, and deterioration of power quality. According to existing literature, the mitigation of SSO can be achieved by employing a flexible AC transmission system (FACTS)[10–12] or by implementing a supplementary damping controller (SDC) in the converters controllers of the DFIG[13,14]. It is important to acknowledge that the FACTS series has been successfully implemented in numerous stations worldwide to facilitate power-flow control and mitigate power oscillation[15].

The thyristor-controlled series capacitor (TCSC), which is the first generation of series controllable compensators, is made up of a fixed capacitor for each phase and a thyristor-controlled reactor (TCR) connected in parallel. The power transfer capacity of the current transmission lines is increased by this device. Numerous scholarly works have examined the use of the TCSC in removing SSO potential dangers. A fixed capacitor and antiparallel reverse blocking semiconductor switches (such as gate turn-off (GTO) thyristor) linked in parallel make up the gate-controlled series capacitor (GCSC), a FACTS device that represents the second generation of series controllable compensators. Different amounts of series compensation may be produced by varying the turn-on period of semiconductor switches. Improved power quality is another benefit of using the GCSC in addition to controlling the power flow of transmission lines. Installing the GCSC over the TCSC may offer certain advantages in several scenarios when using a controlled series compensator is deemed desirable. Table.1 below provides examples of reported literature that utilized FACTs in the mitigation of SSO.

Existing literature suggests that the proportional-integral (PI) controller, despite its widespread adoption due to its ease of implementation and user-friendliness, may exhibit limitations in ensuring stability during abnormal grid conditions within DFIG-based wind plants. The IEEE benchmark model itself reflects this selection, primarily valuing simplicity over robustness. Recent advancements have seen the proportional resonant (PR) controller emerge as a potential alternative to the PI controller in grid-connected current control applications. The PR controller's versatility shines in a wide range of applications, from controlling voltage source inverters[28–31] and active power filters[32,33] to managing electric railway traction systems[34]. Studies have demonstrated that the PR controller offers superior performance under abnormal grid scenarios compared to the PI controller, potentially addressing the stability concerns associated with the latter. This shift presents an opportunity for further research and exploration into the potential benefits of integrating the PR controller within the control strategies of DFIG-based wind plants, particularly in light of increasing demands for grid resilience and power quality.

The main contributions of this research can be succinctly summarized as follows:

(i) This study proposes the synergistic integration of a proportional-resonant (PR) controller with a well-established proportional-integral (PI) controller to generate an optimal turn-off angle for superior damping of sub-synchronous oscillations (SSOs).
(ii) The efficacy of the proposed control strategy is rigorously assessed through time-domain simulations across a spectrum of compensation levels, variable wind speeds, and instances of sub-synchronous control interaction (SSCI).
(iii) A comprehensive comparative analysis is conducted to evaluate the proposed method's effectiveness and robustness in damping SSOs. This analysis compares the proposed method against established techniques such as supplementary damping control (SDC) and a standalone PI controller.

Refs.	FACTs device	Utilized controller/ Approach	Remarks
[16]	TCSC	PI controller	The authors investigated the appropriate parameters of TCSC Investigation of the proper synchronization signal
[17]	TCSC	Proportional resonance with harmonic compensators (PR + HC)	Coordinated design of PR + HC with TCSC
[18]	Static synchronous compensator (STATCOM)	PI controller	Instability can result from the SSO caused by the IGE being visible when the transmission system resistance is reduced
[19]	GCSC	PI controller	There is a crucial for using an auxiliary damping controller with the GCSC
[20]	Static synchronous series compensator (SSSC)	Fuzzy logic control	Reduction in steady state error and increased damping ability
[21]	Static var compensator (SVC)	Adaptive neuro-fuzzy inference systems (ANFIS)	The ANFIS's ability to damp SSR and low-frequency oscillations
[22]	SVC	Fractional sliding mode control	The proposed controller quickly mitigates SSCI and increases system resilience at the same time
[23]	Voltage source converter-based HVDC	PI controller	Mitigation of the torsional oscillation and equipment interaction
[24]	Unified power flow controller (UPFC)	PI controller	Proposes UPFC's novel control strategy Enhanced damping capability
[25]	GCSC	Takagi–Sugeno fuzzy control	Cost-effective solution for SSO damping
[26]	GCSC	PI controller	Using additional supplementary damping control signal
[27]	GCSC	Turn off angle generation based on frequency and maximum voltage value estimation	Fast response and simple implementation

Table 1. Sample of reported literature that utilized FACTS in SSO alleviation.

This paper is organized into six sections. Section "GCSC description" delves into a detailed description of the GCSC, providing a thorough understanding of its components and functionalities. Section "Proposed control approach" then shifts focus to the proposed methodology. Subsequently, Sect. "IEEE test system" presents the power system model employed in the research. Section "Simulation outcomes and discussion" unveils the simulation results and engages in insightful discussions to elucidate their significance. Finally, Sect. "Conclusion" succinctly summarizes the key findings and outcomes of the conducted research.

GCSC description

Figure 1 shows the GCSC block diagram. It comprises a fixed capacitor (X_C) connected in parallel with a pair of GTO thyristors. The capacitor current, line current, and GTO thyristor current are represented, respectively, by the variables I_C, I_{Line}, and I_{GTO}. The line current's zero crossings are used to calculate the turn-off angle (γ).

The effective reactance of the GCSC (X_{GCSC}) in respect to the turn-off angle is shown in Fig. 2. It is feasible to compute this reactance in this way:

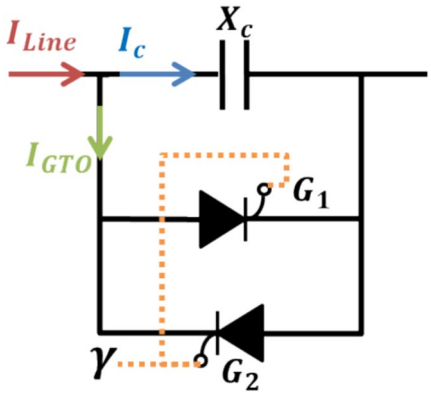

Fig. 1. GCSC configuration.

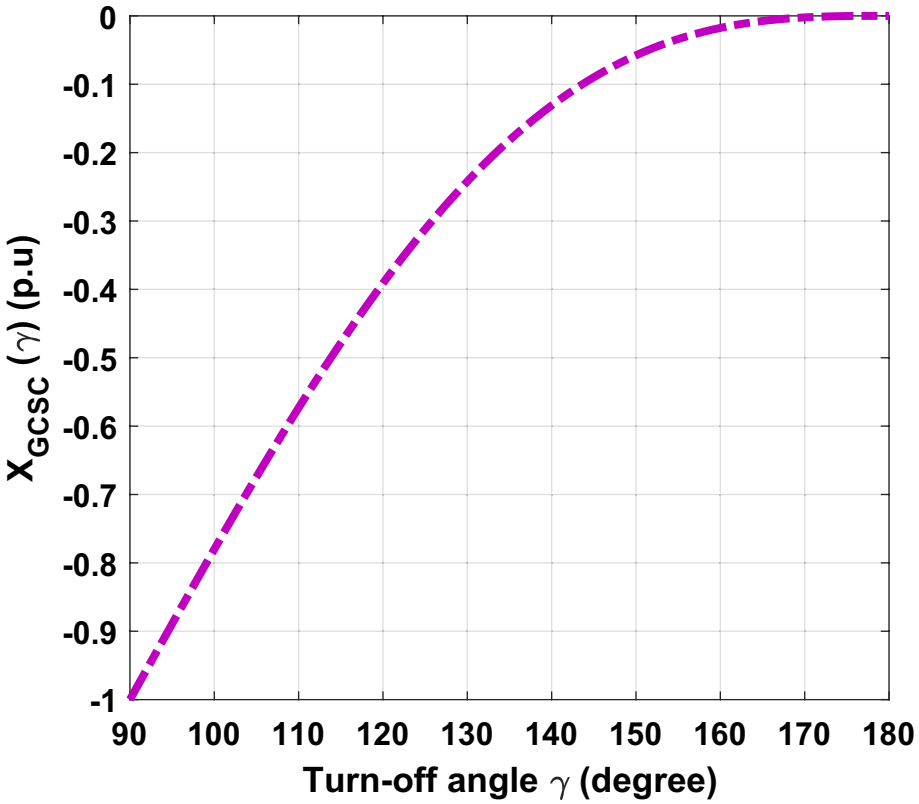

Fig. 2. GCSC reactance with respect to turn-off angle.

$$X_{GCSC}(\gamma) = \frac{X_C}{\pi}(2\gamma - 2\pi - \sin(2\gamma)) \quad (1)$$

Figure 2 shows the relation between the turn-off angle and GCSC reactance. It is clear that as the turn-off angle changes from 90° to 180, X_{GCSC} declines gradually from 1.0, the capacitor is fully integrated into the circuit, to zero, the capacitor is entirely eliminated from the circuit. In other words, the higher the turn-off angle, the lower the X_{GCSC}, and thus the lower the total compensation level (Fixed series capacitor plus X_{GCSC}). That is to say, by changing the turn-off angle, the total compensation level changes, affecting the system's stability. It is worth to be mentioned that, the higher the compensation level, the lower the system stability[35].

Proposed control approach

Figure 3 illustrates the block diagram of the active power regulation of the GCSC. Within this diagram, T_m represents the time constant of a first-order low-pass filter that is linked to the measurement of the DFIG output power. Both the measured and reference active powers are required. First, the P_{meas} is the active power flowing in the transmission line and can be calculated by measuring the voltage and current at the GCSC[25]. Second, the wind speed at the WTG is needed to communicate with the GCSC to obtain the P_{ref}, as previously introduced in many research papers[26,36]. The Lookup table is used to obtain the P_{ref} at a given wind speed. The resulting error is then fed into a proportional-integral (PI) regulator whose gains are K_p and K_I to generate the suitable turn-off angle. In this study, $K_P = 20$, and $K_I = 10$. This method cannot mitigate the SSO within a wide range of compensation levels and wind speeds because the generated turn-off angle is less than the required value[25,37].

To overcome this issue, an additional supplementary damping controller (SDC) is integrated into the CPC approach, as shown in Fig. 4. The SDC is a proportional controller whose input signal and gain are I_{Line} and K_{SDC}, respectively[26,37]. The main goal of SDC is to increase the turn-off angle which in turn leads to cancel part of the compensation level and thus maintain the system stability.

With the traditional method (PI + SDC)[26], at low wind speed or high compensation level, the higher turn-off angle is generated to reduce the total compensation level which in turn makes the system stable. In this study, $K_{SDC} = 26$, $K_P = 20$, and $K_I = 10$. Even so, the PI controller encounters certain limitations in terms of sensitivity towards parametric variables and dynamic conditions. For instance, when faced with significant disturbances, the PI controller's anti-windup capability becomes compromised[17].

The PI controller is widely employed due to its relative ease of implementation. This simplicity facilitates control and filtering within the system. However, PI controllers exhibit limitations. Firstly, their performance suffers from cross-coupling between the "d" and "q" components in rotating reference frame control methods. This necessitates the introduction of decoupling terms and voltage feedforward to enhance performance[38]. Secondly, PI controllers struggle to eliminate low-order harmonics, which can be problematic in grid-connected applications[39].

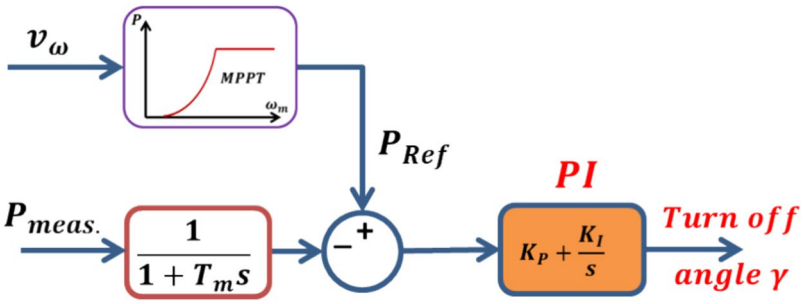

Fig. 3. Generation of turn-off angle using PI controller[25].

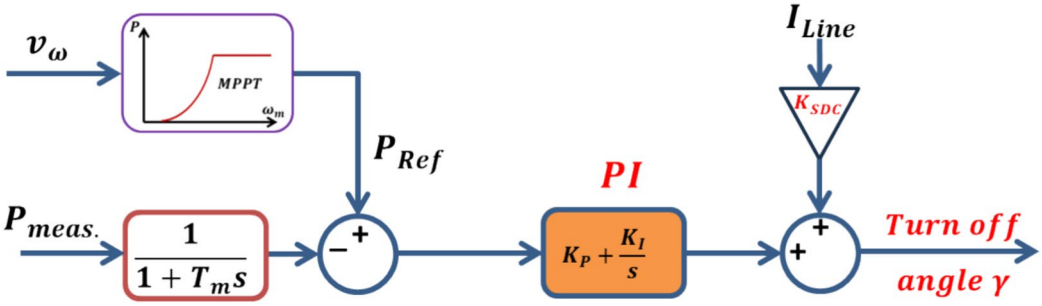

Fig. 4. Generation of turn-off angle using PI controller with the aid of SDC[26].

The PR controller emerges as a promising alternative to the PI controller. Combining a proportional term with a resonant term, the PR controller offers several advantages. One key benefit is its ability to eliminate steady-state error by providing additional gain at the specific resonant frequency of the controlled signal[40]. Additionally, the PR controller offers the capability to integrate a harmonic compensator (HC) without compromising dynamic control, leading to high-quality current control[41]. Furthermore, the complexity of current control is reduced by employing a stationary reference frame compared to the synchronous reference frame "dq" method. This is because Park's transformation, a source of complexity, is no longer required. Importantly, currents in the alpha–beta (α–β) coordinates of the stationary frame are not cross-coupled, eliminating the need for decoupling circuitry[42]. Finally, the PR control can function as a notch filter to compensate for harmonics within the control signal[38]. Therefore, the PR controller was utilized in several applications such as controlling voltage source inverters[28], and active power filters[32]. Moreover, cascaded predictive-integral-resonant controllers were used for disturbance attenuation of permanent magnet synchronous motors[43].

In the proposed method, the ability of the cascaded PR-PI controller to dampen the SSO is investigated. The PR controller can be mathematically described as follows:

$$G_{PR}(s) = k_p + \frac{2k_i\omega_c s}{s^2 + 2\omega_c s + \omega_0^2} \tag{2}$$

where k_p, k_i are the proportional and resonant factors, respectively and ω_c is the cut-off frequency of the quasi-resonant controller. As illustrated in Fig. 5, the error signal generated by subtracting the measured active power from the reference active power is fed into the PR controller. The output of the PR controller is then used as the input for the PI controller.

The control performance of the resonant controller depends on these factors. The proper values for k_p, k_i, and ω_c were chosen by trial and error in order to develop the PR controller. This control structure parameres has to be carefully set to ensure its damping capability. Table 2 provides the parameter values for the controllers as utilized in this research.

IEEE test system

To investigate sub-synchronous resonance (SSR) behavior in DFIG-based wind farms, the original IEEE benchmark platform was modified by replacing the synchronous machine with a DFIG wind plant. This research utilizes a 100 MW wind farm composed of 67 individual 1.5 MW turbines. The DFIG's output voltage of 575 V

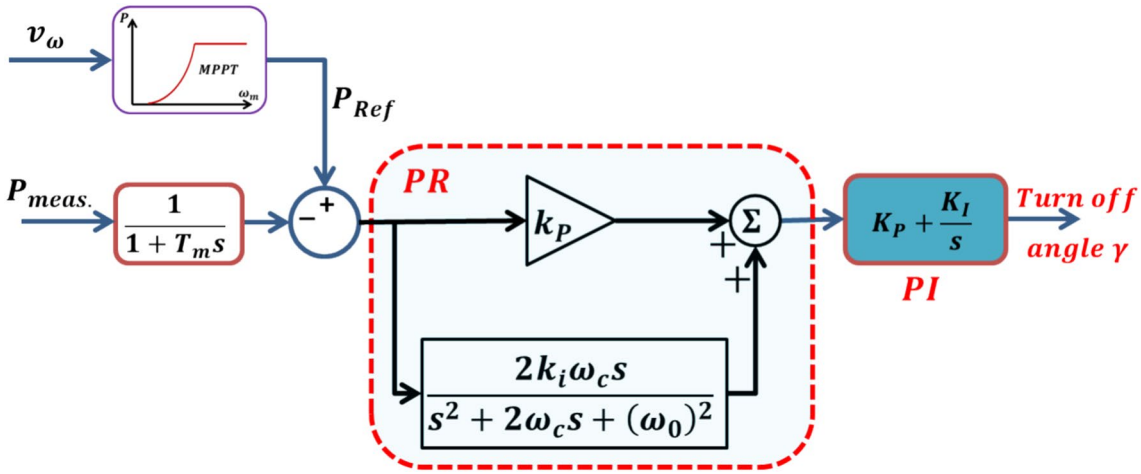

Fig. 5. Generation of turn-off angle using the proposed method (PR–PI controllers).

Parameters	Value
PR controller	
k_p	20
k_i	10
ω_0	900
ω_c	0.8
PI controller	
K_P	20
K_I	10

Table 2. Parameters for the proposed method (PR–PI controller).

is connected to a 161 kV series capacitor transmission line via a step-up transformer, enabling integration with the infinite bus as depicted in Fig. 6. The transmission line series impedance is denoted by $Z_L = R_L + jX_L$, where X_{FC} denotes the fixed series compensation capacitor. To perform SSR analysis on this modified system, a previously published mathematical model for DFIG-based wind farms was employed, with parameter values readily available in the literature[9,35,44–47].

Simulation outcomes and discussion

This section leverages MATLAB/Simulink software to conduct a time-domain simulation, thereby validating the proposed approach's superiority and effectiveness in mitigating the SSO phenomenon compared to the conventional methods. In a DFIG-based wind farm interfaced with a series-compensated network, there are only two types of oscillation because of the low shaft stiffness coefficient of the DFIG-wind turbine, namely, induction generator effect (IGE) that occurs due to the high compensation level or low wind speed, and sub-synchronous control interaction (SSCI)[2,13,48]. IGE occurs because of the interaction between the series-compensated transmission line and rotor electrical dynamic of DFIG. Thus, IGE is purely an electrical phenomenon. Whereas SSCI occurs due to the interaction between power electronic devices (DFIG controllers) and a series capacitor of the transmission line[48].

Different series compensation level

Initially, the system is stable where the compensation level is low (10%), and the wind speed is held constant at 7 m/s. Then, at $t = 15$ s, the compensation level is increased to 40%, 50%, and 60% as shown in Figs. 7, 8, and 9, respectively. Without a controller, it is clear from Figs. 7, 8, and 9 that the higher the compensation level, the higher the electrical natural frequency, f_n, or lower sub-synchronous frequency f_{sso}. Thus, the lower the sub-synchronous slip value, $S_{SSR} = \frac{f_n - f_m}{f_n}$, which in turn makes the equivalent rotor resistance, R_r/S_{SSR}, exceeds the total resistance of the armature and network[35]. Therefore, the oscillation appears and the system becomes more unstable as the compensation level increases. It should be noted that f_{sso} is the difference between the fundamental frequency and the electrical natural frequency $(f_{sso} = f_s - f_n)$. From Figs. 7, 8, and 9, $f_{sso} = 32$ Hz, 28.5 Hz, and 25.5 Hz for K = 40%, 50%, and 60%, respectively.

The performance of the previous methods[25,26] and the proposed method for damping the oscillation is displayed in Figs. 7, 8, 9, and 10. With the PI controller[25], the oscillation is completely damped after around 1.6 s at a 40% compensation level as shown in Fig. 7a, whereas the system lacks stability at higher compensation levels where the oscillation ranges from − 0.23 to − 0.3 p.u. for $K = 50\%$, and ranges from − 0.21 to − 0.32 p.u. for $K = 60\%$, as shown in Figs. 8a and 9a, respectively. On the other hand, the same performance is achieved by Ref[26] and the proposed method at 40% compensation level, where they consume roughly 0.25 s to reach the steady state. Whereas the proposed method achieves faster convergence at 50% and 60% compensation levels compared to Ref[26], where the proposed method consumes 0.25 s while[26] takes around 0.45 s to reach the steady state as shown in Figs. 8b and 9b. Also, it can be observed that the overshoots provided by the proposed method are almost equally or slightly greater than that of Ref[26].

Variable wind speed

Initially, the system operates at a low compensation level (10%). The wind speed is set to 9 m/s in Fig. 10, and 11 m/s in Fig. 11. Then, at $t = 15$ s, a high compensation level is increased to 60% in all studied cases. Since the compensation level equals 60% in the two studied cases, the f_{sso} equals 25.5 Hz in the two cases as shown in Figs. 10a and 11a. Given that the wind speed increases, the DFIG rotor speed increases, and thus the electrical frequency, f_m, increases. Thus, the sub-synchronous slip value becomes higher, and thus the equivalent rotor resistance is less than the total resistance of the armature and network[35]. Therefore, the amplitude of oscillation is lower, where it ranges from − 2 to 0.8 p.u. for 9 m/s wind speed and ranges from − 1.2 to 0.1 p.u. for 11 m/s wind speed, as shown in Figs. 10a and 11a. The performance of the previous methods[25,26] and the proposed method for mitigating the SSO is illustrated in Figs. 10 and 11.

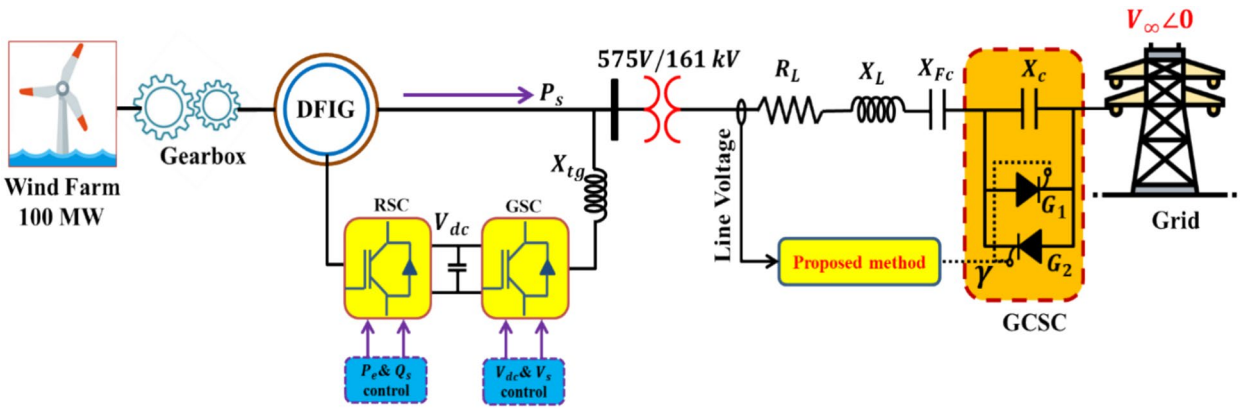

Fig. 6. The IEEE test system.

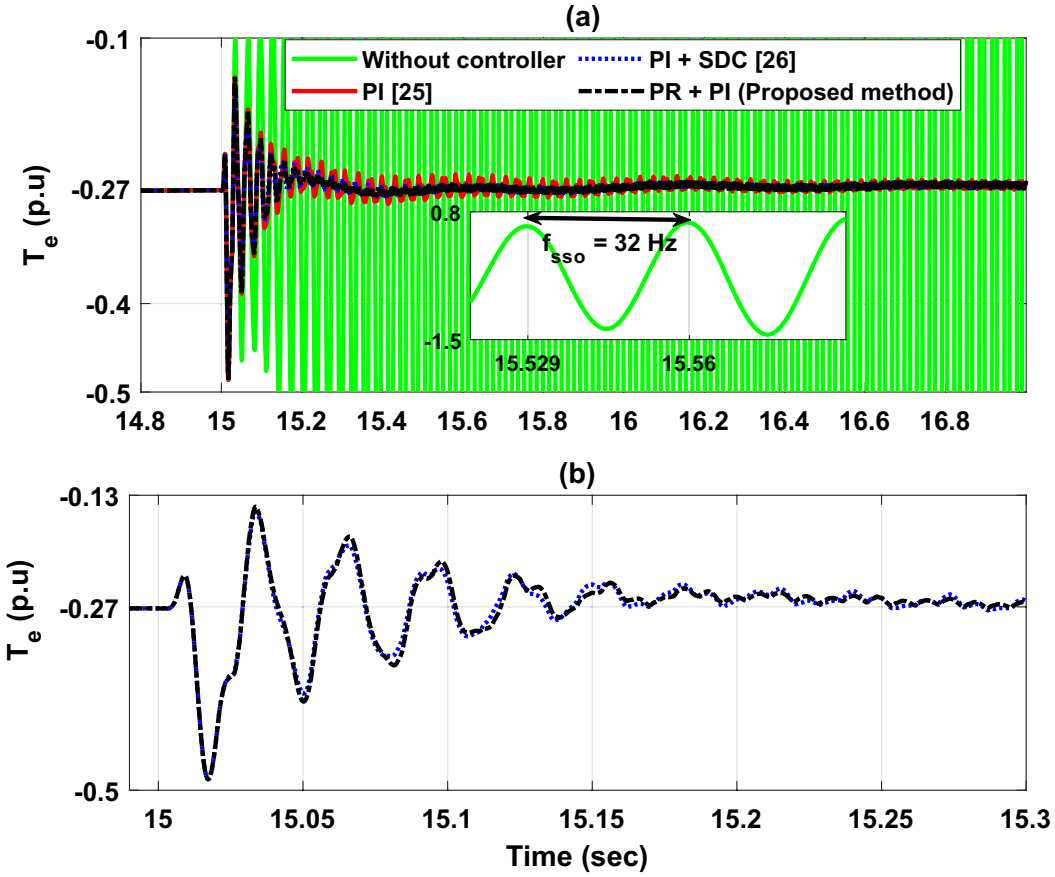

Fig. 7. The DFIG output torque response at a wind speed of 7 m/s and a compensation level of 40%.

As shown in Figs. 10a and 11a, the PI controller[25] can damp the oscillation after around 2.5 s and 0.6 s for 9 m/s and 11 m/s wind speed, respectively. This proves that the system becomes more stable as the wind speed increases. On the other hand, it can be noted a better performance is achieved by the proposed method at lower wind speeds, as shown in Figs. 9b and 10b, while the PI + SDC[26] provides less overshot compared to the proposed method at 11 m/s wind speed, as shown in Fig. 11b.

Figure 12 shows the impact of increasing the wind speed gradually from 9 to 11 m/s. It is clear that the system is stable, and the previous and the proposed methods have the same performance.

Sub-synchronous control interaction

The SSCI is the most hazardous type of SSO, where the oscillation grows too quickly due to the interaction between the series-compensated transmission line and the DFIG controllers. To simulate the SSCI, a relatively low wind speed (7 m/s), a high compensation level (60%), and a three-phase-to-ground-fault (LLLG) are applied. The LLLG fault is created when $t = 15$ s at the high voltage side of the coupling transformer and lasts for 200 ms. As depicted in Fig. 13, the system suffers from a big disturbance when there is no controller. It is clear that both[26] and the proposed method roughly have the same performance, where they have the same oscillation amplitude, as shown in Fig. 13b. Also, it is observed that the oscillation amplitude by Ref[25] is greater than[26] and the proposed method.

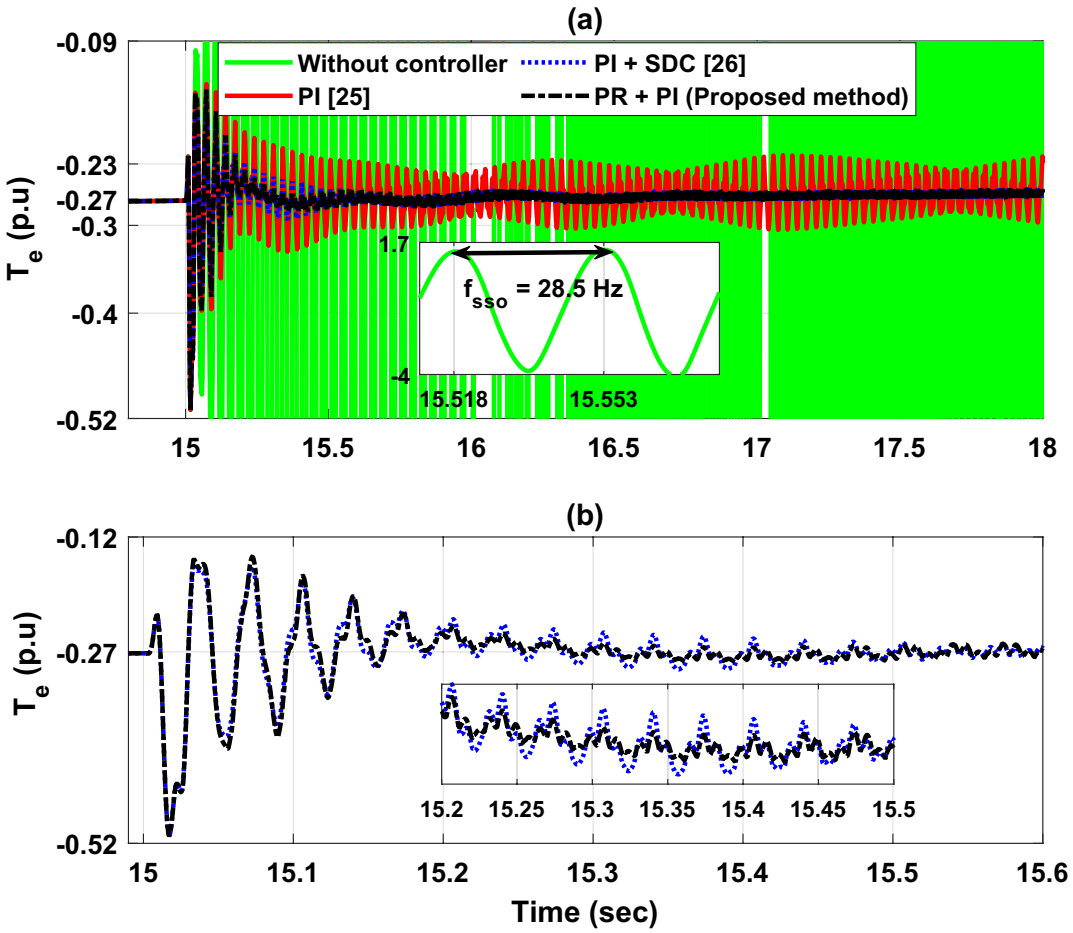

Fig. 8. The DFIG output torque response at a wind speed of 7 m/s and a compensation level of 50%.

Conclusion

In this paper, the ability of the cascaded PR controller with a PI controller for mitigating the SSO is investigated in a DFIG-based wind farm interfaced with a series-compensated network. This combined approach aims to achieve an optimal turn-off angle, leading to better SSO damping and enhancing the system's stability. To meticulously evaluate the effectiveness of this control strategy, extensive time-domain simulations were conducted within a wide range of the compensation levels and wind speeds as well as SSO caused by SSCI. The results demonstrated: (1) that the proposed method can successfully damp the SSO at different operating points with different oscillation frequencies. (2) The superiority and effectiveness of the proposed method compared to the PI controller technique, where the least settling time is observed. (3) That faster convergence is achieved by the proposed method at high compensation levels and low wind speeds compared to the PI+SDC technique. (4) The cascaded PR-PI controller can be used instead of the PI+SDC controller for damping the SSO. Moreover, the adaptability of the proposed method for different grid strengths, using recent optimization methods for selecting the optimum parameters of the proposed method, and its test practically will be the subject of future works.

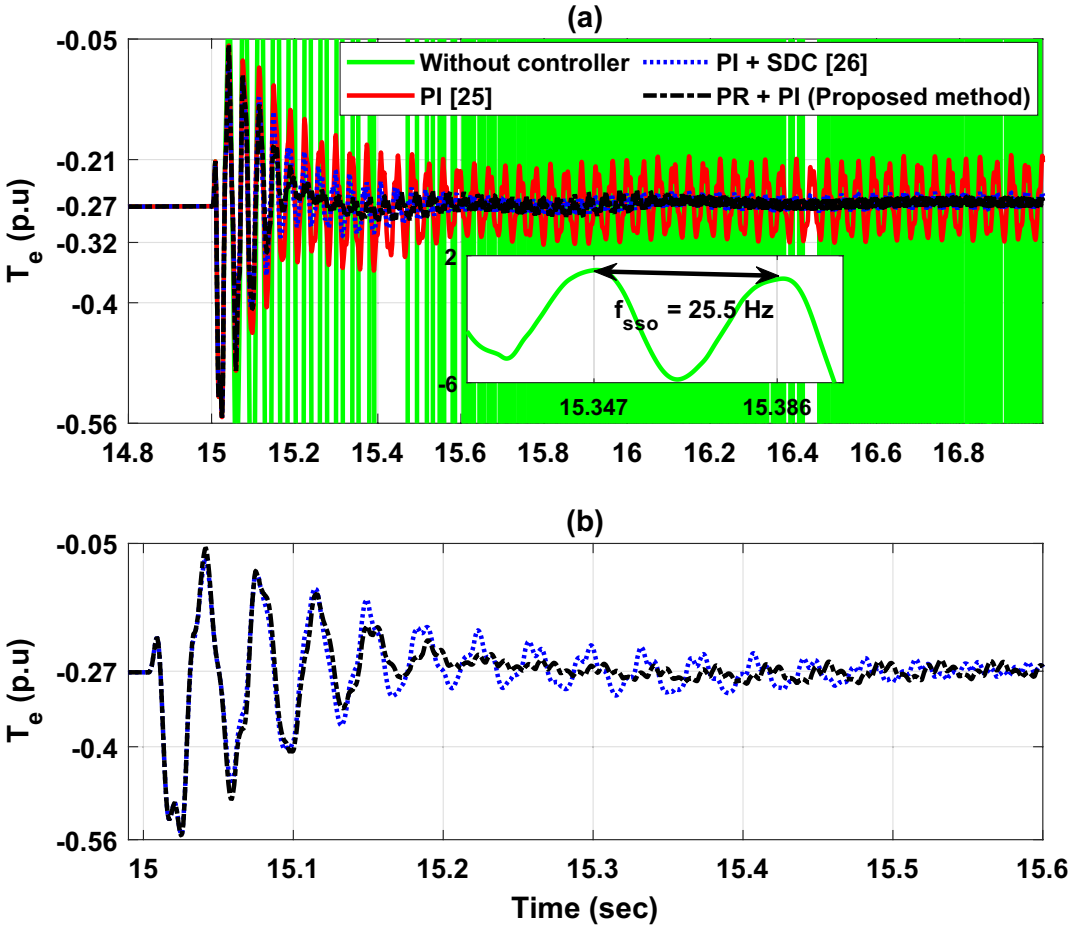

Fig. 9. The DFIG output torque response at a wind speed of 7 m/s and a compensation level of 60%.

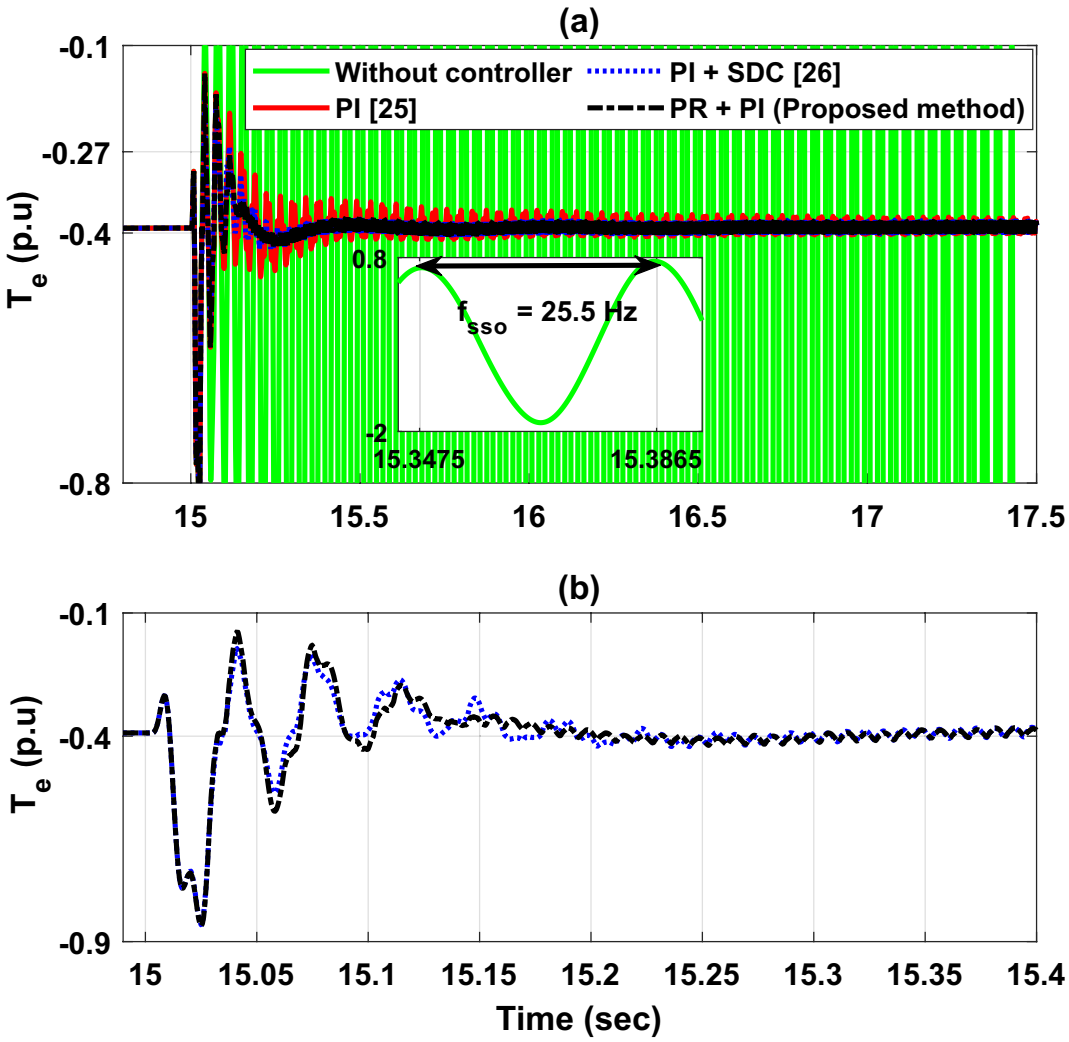

Fig. 10. The DFIG output torque response at a wind speed of 9 m/s and a compensation level of 60%.

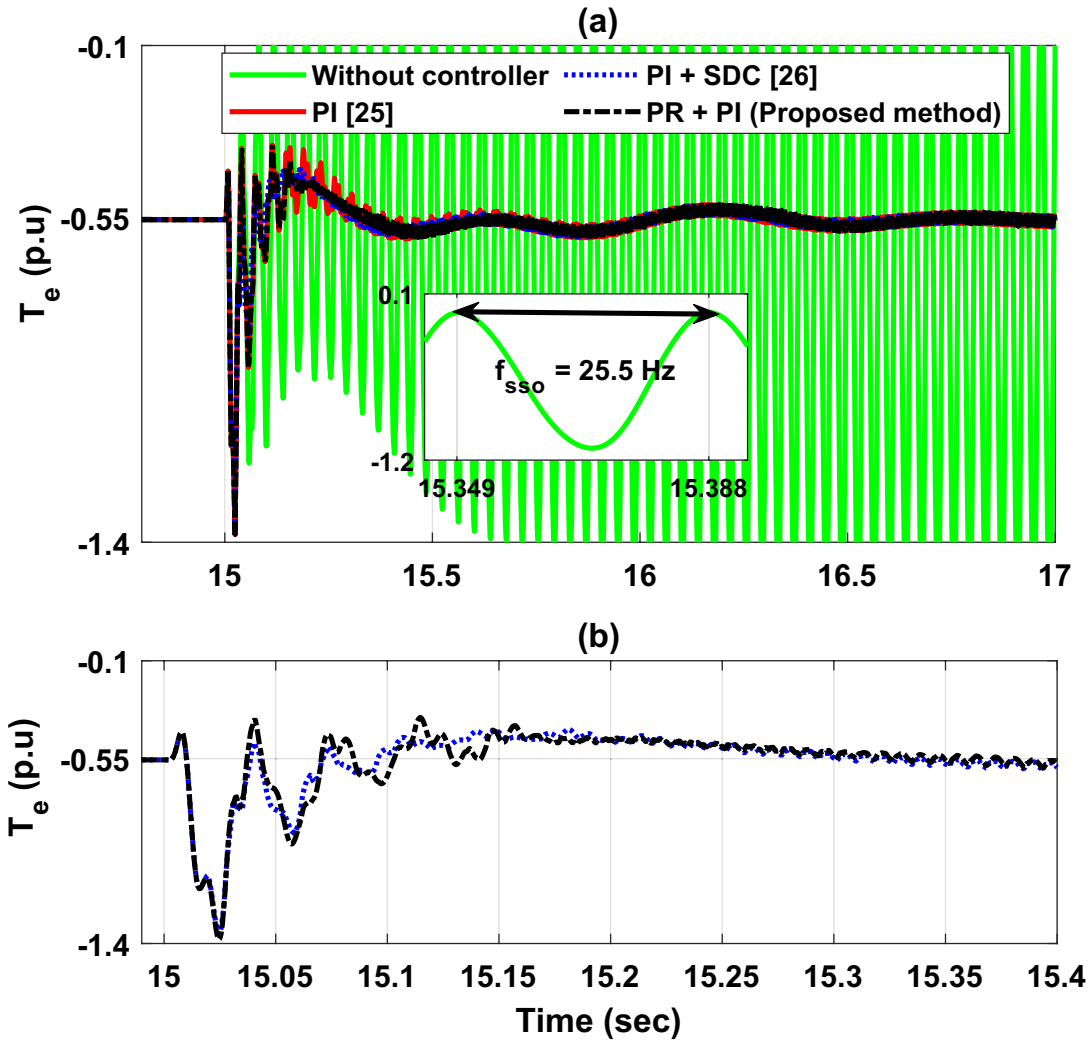

Fig. 11. The DFIG output torque response at a wind speed of 11 m/s and a compensation level of 60%.

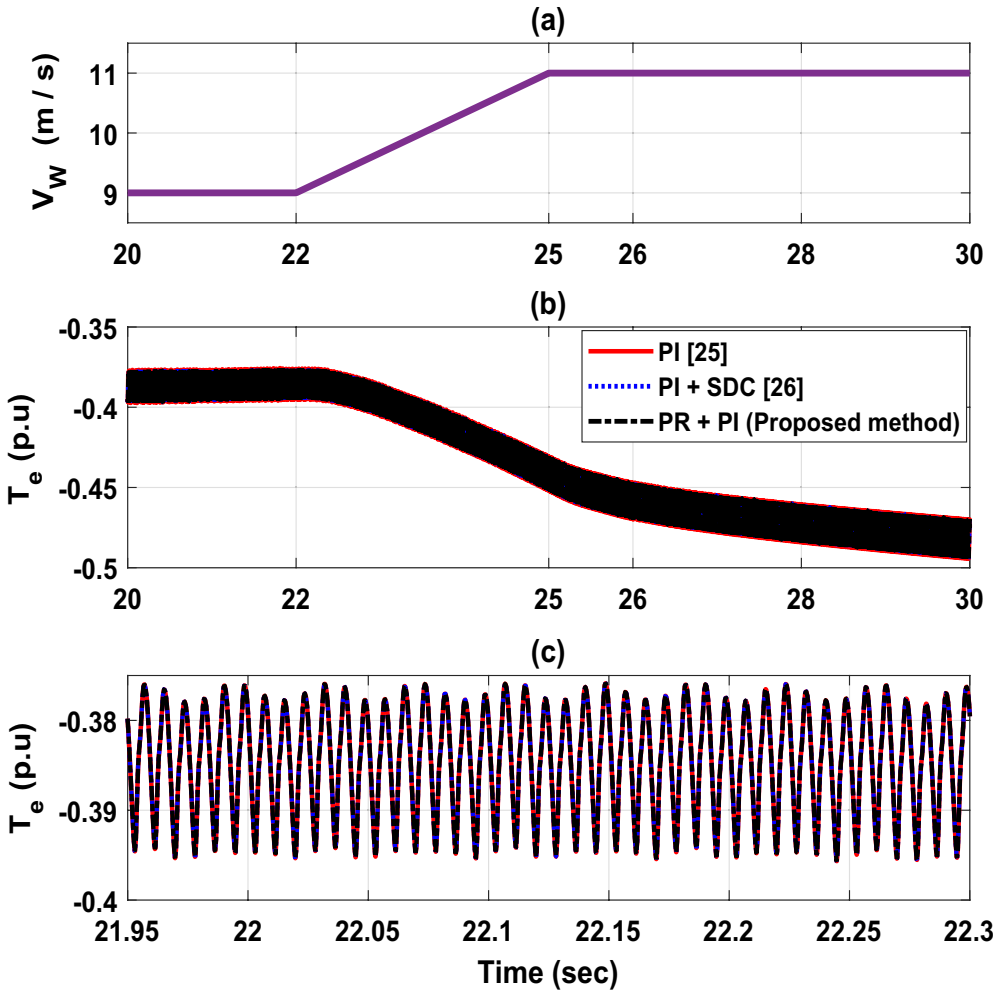

Fig. 12. The DFIG output torque response when the wind speed increases gradually from 9 to 11 m/s and the compensation level equals 60%.

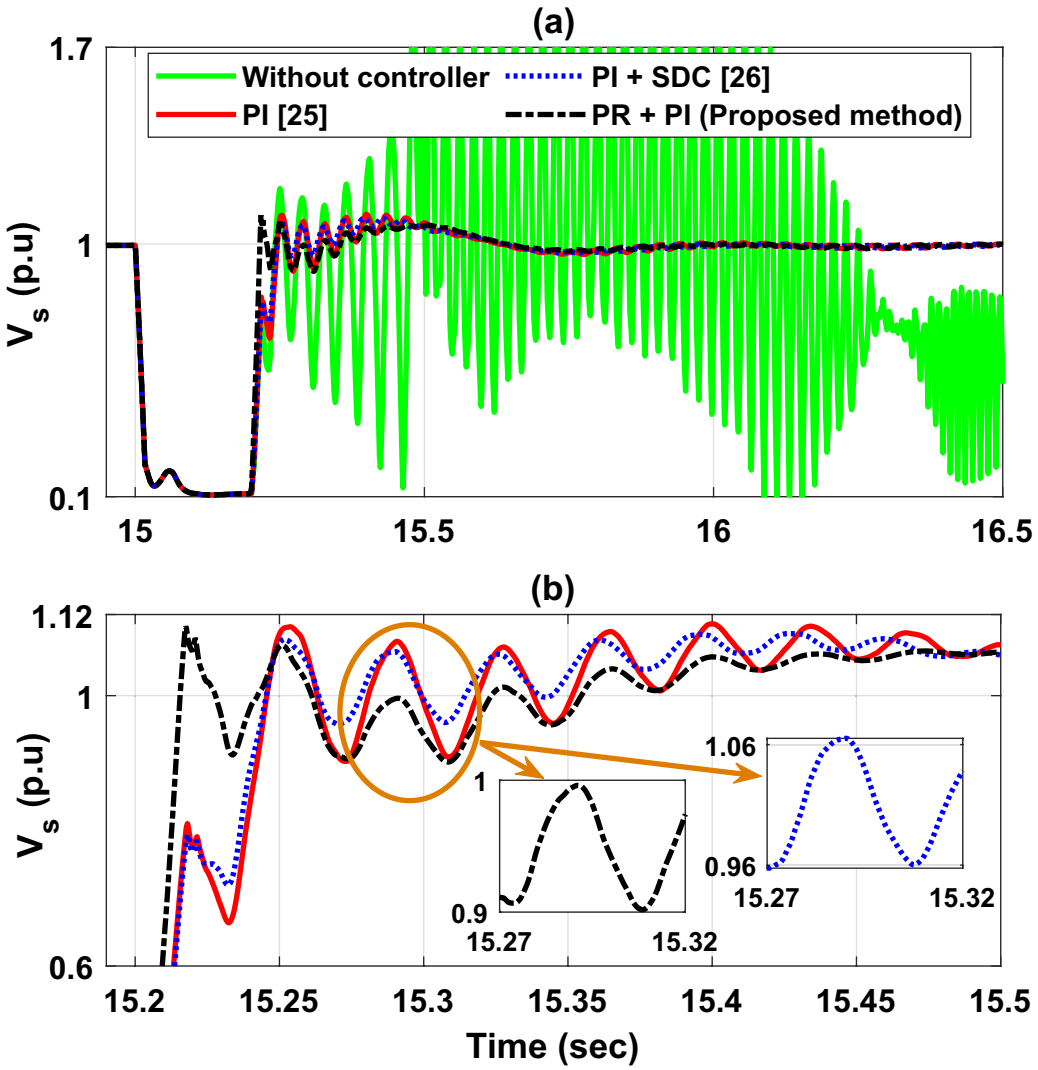

Fig. 13. The DFIG terminal voltage response during the SSCI.

Data availability

"All data generated or analyzed during this study are included in this published article[and its supplementary information files]. https://ieeexplore.ieee.org/document/9416650.

Received: 4 March 2024; Accepted: 3 September 2024
Published online: 04 December 2024

References

1. Nilsson, S. *et al. Application Examples of the Thyristor Controlled Series Capacitor* 1–59 (Springer, Switzerland, 2019).
2. Xie, X. *et al.* Characteristic analysis of subsynchronous resonance in practical wind farms connected to series-compensated transmissions. *IEEE Trans. Energy Convers.* **32**(3), 1117–1126. https://doi.org/10.1109/TEC.2017.2676024 (2017).
3. Gu, K., Wu, F. & Zhang, X. Sub-synchronous interactions in power systems with wind turbines: A review. *IET Renew. Power Gener.* **13**(1), 4–15. https://doi.org/10.1049/iet-rpg.2018.5199 (2019).
4. Karaagac, U. *et al.* Safe operation of DFIG-based wind parks in series-compensated systems. *IEEE Trans. Power Deliv.* **33**(2), 709–718. https://doi.org/10.1109/TPWRD.2017.2689792 (2018).
5. He, C., Sun, D., Song, L. & Ma, L. Analysis of subsynchronous resonance characteristics and influence factors in a series compensated transmission system. *Energies* **12**(17), 3282. https://doi.org/10.3390/en12173282 (2019).
6. Verma, N., Kumar, N., Gupta, S., Malik, H. & García Márquez, F. P. Review of sub-synchronous interaction in wind integrated power systems: Classification, challenges, and mitigation techniques. *Prot. Control Mod. Power Syst.* **8**(1), 17. https://doi.org/10.1186/s41601-023-00291-0 (2023).
7. Perera, U., Oo, A. M. T. & Zamora, R. Sub synchronous oscillations under high penetration of renewables—a review of existing monitoring and damping methods, challenges, and research prospects. *Energies* **15**(22), 8477. https://doi.org/10.3390/en15228477 (2022).
8. Tsebia, M. & Bentarzi, H. Sub-synchronous torsional interaction study and mitigation using a synchro-phasors measurement unit. in *ICCEIS 2021*, Basel Switzerland: MDPI, p. 8. https://doi.org/10.3390/engproc2022014008 (2022).

9. Fan, L., Kavasseri, R., Miao, Z. L. & Zhu, C. Modeling of DFIG-based wind farms for SSR analysis. *IEEE Trans. Power Deliv.* **25**(4), 2073–2082. https://doi.org/10.1109/TPWRD.2010.2050912 (2010).
10. Duc Tung, D., Van Dai, L. & Cao Quyen, L. Subsynchronous resonance and FACTS-novel control strategy for its mitigation. *J. Eng.* **2019**, 1–14. https://doi.org/10.1155/2019/2163908 (2019).
11. Golshannavaz, S., Aminifar, F. & Nazarpour, D. Application of UPFC to enhancing oscillatory response of series-compensated wind farm integrations. *IEEE Trans. Smart Grid* **5**(4), 1961–1968. https://doi.org/10.1109/TSG.2014.2304071 (2014).
12. Bhowmick, S. *Flexible AC Transmission Systems (FACTS): Newton Power-Flow Modeling of Voltage-Sourced Converter-Based Controllers* (CRC Press, Cham, 2018).
13. Abdeen, M. *et al.* Sub-synchronous interaction damping controller for a series-compensated DFIG-based wind farm. *IET Renew. Power Gener.* **16**(5), 933–944. https://doi.org/10.1049/rpg2.12400 (2022).
14. Karunanayake, C., Ravishankar, J. & Dong, Z. Y. Nonlinear SSR damping controller for DFIG based wind generators interfaced to series compensated transmission systems. *IEEE Trans. Power Syst.* **35**(2), 1156–1165. https://doi.org/10.1109/TPWRS.2019.2938230 (2020).
15. Qader, M. R. Use of FACTS devices in mitigating subsynchronous resonance. *Adv. Electr. Electron. Eng.* **18**(2), 57–64. https://doi.org/10.15598/aeee.v18i2.2997 (2020).
16. Abdeen, M. *et al.* Investigation on TCSC parameters and control structure for SSR damping in DFIG-based wind farm. in *2021 12th Int. Renew. Energy Congr. IREC 2021*, no. Irec, pp. 3–7. https://doi.org/10.1109/IREC52758.2021.9624934 (2021).
17. Islam, S. U. & Kim, S. Design and implementation of optimal control scheme for DFIG based wind plant to mitigate sub-synchronous resonance issues. *IEEE Access* **11**(December), 141162–141171. https://doi.org/10.1109/ACCESS.2023.3341884 (2023).
18. Nagarajan, S.T. & Kumar, N. Mitigation of induction generator effect due to SSR with STATCOM in synchronous generator. in *2012 IEEE 5th India International Conference on Power Electronics (IICPE)*, IEEE, Dec. 2012, pp. 1–6. https://doi.org/10.1109/IICPE.2012.6450444 (2012).
19. Emarloo, A. A., Changizian, M. & Shoulaie, A. Application of gate-controlled series capacitor to mitigate subsynchronous resonance in a thermal generation plant connected to a series-compensated transmission network. *Int. Trans. Electr. Energy Syst.* **30**(12), 1–20. https://doi.org/10.1002/2050-7038.12673 (2020).
20. Prasad, C. E. & Vadhera, S. Fuzzy logic based SSSC as sub-synchronous resonance damping controller. in *2015 International Conference on Energy, Power and Environment: Towards Sustainable Growth (ICEPE)*, IEEE, Jun. 2015, pp. 1–4. https://doi.org/10.1109/EPETSG.2015.7510175 (2015).
21. Amirian, M. Mitigating sub-synchronous resonance using static var compensator (SVC) enhanced with adaptive neuro-fuzzy inference systems (ANFIS) controller. in *2019 27th Iranian Conference on Electrical Engineering (ICEE)*, IEEE, Apr. 2019, pp. 532–538. https://doi.org/10.1109/IranianCEE.2019.8786701 (2019).
22. Li, P. *et al.* Mitigating subsynchronous control interaction using fractional sliding mode control of wind farm. *J. Franklin Inst.* **357**(14), 9523–9542. https://doi.org/10.1016/j.jfranklin.2020.07.024 (2020).
23. Zhou, Q., Ding, Y., Mai, K., Bian, X. & Zhou, B. Mitigation of subsynchronous oscillation in a VSC-HVDC connected offshore wind farm integrated to grid. *Int. J. Electr. Power Energy Syst.* **109**(August), 29–37. https://doi.org/10.1016/j.ijepes.2019.01.031 (2018).
24. Zhu, X. *et al.* Subsynchronous resonance and its mitigation for power system with unified power flow controller. *J. Mod. Power Syst. Clean Energy* **6**(1), 181–189. https://doi.org/10.1007/s40565-017-0283-2 (2018).
25. Alizadeh Pahlavani, M. R. & Mohammadpour, H. A. Damping of sub-synchronous resonance and low-frequency power oscillation in a series-compensated transmission line using gate-controlled series capacitor. *Electr. Power Syst. Res.* **81**(2), 308–317. https://doi.org/10.1016/j.epsr.2010.09.007 (2011).
26. Mohammadpour, H. A. & Santi, E. Modeling and control of gate-controlled series capacitor interfaced With a DFIG-based wind farm. *IEEE Trans. Ind. Electron.* **62**(2), 1022–1033. https://doi.org/10.1109/TIE.2014.2347007 (2015).
27. Abdeen, M., El-Dabah, M. A., Domínguez-García, J. L. & Kamel, S. Gate-controlled series capacitor: A new methodology for mitigating sub-synchronous resonance in a series-compensated DFIG-based wind farm. *IET Renew. Power Gener.* **17**(10), 2638–2647. https://doi.org/10.1049/rpg2.12776 (2023).
28. Haro-Larrode, M., Santos-Mugica, M., Eguia, P., Rodriguez-Sanchez, R. & Gil-de-Muro, A. Impact of proportional resonant controller parameters of VSC connected to AC grids with variable X/R characteristic on the small signal stability. *Int. J. Electr. Power Energy Syst.* **118**(October), 105746. https://doi.org/10.1016/j.ijepes.2019.105746 (2020).
29. Kalaiselvi, P., Chenthur Pandian, S. & Anand, M. Enhanced proportional resonant—second-order general integrators (EPR-SOGI) with fuzzy logic control in hybrid renewable energy source-based STATCOM. *Electr. Power Compon. Syst.* https://doi.org/10.1080/15325008.2024.2332396 (2024).
30. Nowak, M., Binkowski, T. & Piróg, S. Proportional-resonant controller structure with finite gain for three-phase grid-tied converters. *Energies* **14**(20), 6726. https://doi.org/10.3390/en14206726 (2021).
31. Ebrahim, M. A., Aziz, B. A., Nashed, M. N. F. & Osman, F. A. Optimal design of proportional-resonant controller and its harmonic compensators for grid-integrated renewable energy sources based three-phase voltage source inverters. *IET Gener. Transm. Distrib.* **15**(8), 1371–1386. https://doi.org/10.1049/gtd2.12108 (2021).
32. Amini, B., Rastegar, H. & Pichan, M. An optimized proportional resonant current controller based genetic algorithm for enhancing shunt active power filter performance. *Int. J. Electr. Power Energy Syst.* **156**, 109738. https://doi.org/10.1016/j.ijepes.2023.109738 (2024).
33. Bianchi, N. & Dai Pre, M. Active power filter control using neural network technologies. *IEE Proc. Electr. Power Appl.* **150**(2), 139–145. https://doi.org/10.1049/ip-epa (2003).
34. Nuca, I. *et al.* Design of proportional-resonant control for current harmonic compliance in electric railway power systems. in *2023 IEEE Symposium on Electromagnetic Compatibility & Signal/Power Integrity (EMC+SIPI)*, Grand Rapids, MI, USA: IEEE, Jul. 2023, pp. 13–17. https://doi.org/10.1109/EMCSIPI50001.2023.10241757 (2023).
35. Abdeen, M. *et al.* A recent analytical approach for analysis of sub-synchronous resonance in doubly-fed induction generator-based wind farm. *IEEE Access* **9**, 68888–68897. https://doi.org/10.1109/ACCESS.2021.3075965 (2021).
36. Mohammadpour, H. A., Islam, M. M., Santi, E. & Shin, Y. J. SSR damping in fixed-speed wind farms using series FACTS controllers. *IEEE Trans. Power Deliv.* **31**(1), 76–86. https://doi.org/10.1109/TPWRD.2015.2464323 (2016).
37. Abdeen, M. *et al.* Adaptive fuzzy supplementary controller for SSR damping in a series-compensated DFIG-based wind farm. *IEEE Access* **11**, 1467–1476. https://doi.org/10.1109/ACCESS.2022.3232983 (2023).
38. Teodorescu, R. & Blaabjerg, F. Flexible control of small wind turbines with grid failure detection operating in stand-alone and grid-connected mode. *IEEE Trans. Power Electron.* **19**(5), 1323–1332. https://doi.org/10.1109/TPEL.2004.833452 (2004).
39. Blaabjerg, F., Teodorescu, R., Liserre, M. & Timbus, A. V. Overview of control and grid synchronization for distributed power generation systems. *IEEE Trans. Ind. Electron.* **53**(5), 1398–1409. https://doi.org/10.1109/TIE.2006.881997 (2006).
40. Castilla, M. Linear current control scheme with series resonant harmonic compensator for single-phase grid-connected photovoltaic inverters. *IEEE Trans. Ind. Electron.* **55**(7), 2724–2733. https://doi.org/10.1109/TIE.2008.920585 (2008).
41. Liserre, M., Teodorescu, R. & Blaabjerg, F. Multiple harmonics control for three-phase grid converter systems with the use of PI-RES current controller in a rotating frame. *IEEE Trans. Power Electron.* **21**(3), 836–841. https://doi.org/10.1109/TPEL.2006.875566 (2006).

42. Teodorescu, R., Blaabjerg, F., Liserre, M. & Loh, P. C. Proportional-resonant controllers and filters for grid-connected voltage-source converters. *IEE Proc. Electr. Power Appl.* **153**(5), 750. https://doi.org/10.1049/ip-epa:20060008 (2006).
43. Zhou, Z., Xia, C., Yan, Y., Wang, Z. & Shi, T. Disturbances attenuation of permanent magnet synchronous motor drives using cascaded predictive-integral-resonant controllers. *IEEE Trans. Power Electron.* **33**(2), 1514–1527. https://doi.org/10.1109/TPEL.2017.2679126 (2018).
44. Huang, P. H., El Moursi, M. S., Xiao, W. & Kirtley, J. L. Subsynchronous resonance mitigation for series-compensated dfig-based wind farm by using two-degree-of-freedom control strategy. *IEEE Trans. Power Syst.* **30**(3), 1442–1454. https://doi.org/10.1109/TPWRS.2014.2348175 (2015).
45. Fan, L. & Miao, Z. Analytical model building for Type-3 wind farm subsynchronous oscillation analysis. *Electr. Power Syst. Res.* **201**, 107566. https://doi.org/10.1016/j.epsr.2021.107566 (2021).
46. Abdeen, M., Ali, M. H., Soliman, A. M. A., Eslami, M. & Kamel, S. Improved methodology for damping sub-synchronous oscillation in a series-compensated DFIG-based wind farm. *IET Gener. Transm. Distrib.* **17**(14), 3333–3341. https://doi.org/10.1049/gtd2.12906 (2023).
47. Shair, J., Xie, X., Yang, J., Li, J. & Li, H. adaptive damping control of subsynchronous oscillation in DFIG-based wind farms connected to series-compensated network. *IEEE Trans. Power Deliv.* **37**(2), 1036–1049. https://doi.org/10.1109/TPWRD.2021.3076053 (2022).
48. Mohammadpour, H. A. & Santi, E. Sub-synchronous resonance analysis in DFIG-based wind farms: Definitions and problem identification-Part I. in *2014 IEEE Energy Conversion Congress and Exposition (ECCE)*, IEEE, Sep. 2014, pp. 812–819. https://doi.org/10.1109/ECCE.2014.6953480 (2014).

Acknowledgements

The authors extend their appreciation to the Deanship of Scientific Research at Northern Border University, Arar, KSA, for funding this research work through the project number "NBU-FFR-2024-2968-02".

Author contributions

Conceptualization, M.A. and M.E.-D.; methodology, M.A.; software, A.A. and M.E.-D.; validation, M.A., M.E.-D. and A.A.; formal analysis, A.A. and M.A.; investigation, M.A. and M.E.-D.; resources, A.A.; writing—original draft preparation, M.E.-D.; writing—review and editing, A.A. and M.E.-D.; visualization, M.A.; funding acquisition, A.A. All authors have read and agreed to the published version of the manuscript.

Funding

This research was funded by the Deanship of Scientific Research at Northern Border University, Arar, KSA, through the project number "NBU-FFR-2024-2968-02".

Competing interests

The authors declare no competing interests.

Additional information

Correspondence and requests for materials should be addressed to M.A.E.-D.